

# RSC Advances



This is an *Accepted Manuscript*, which has been through the Royal Society of Chemistry peer review process and has been accepted for publication.

*Accepted Manuscripts* are published online shortly after acceptance, before technical editing, formatting and proof reading. Using this free service, authors can make their results available to the community, in citable form, before we publish the edited article. This *Accepted Manuscript* will be replaced by the edited, formatted and paginated article as soon as this is available.

You can find more information about *Accepted Manuscripts* in the [Information for Authors](#).

Please note that technical editing may introduce minor changes to the text and/or graphics, which may alter content. The journal's standard [Terms & Conditions](#) and the [Ethical guidelines](#) still apply. In no event shall the Royal Society of Chemistry be held responsible for any errors or omissions in this *Accepted Manuscript* or any consequences arising from the use of any information it contains.

Cite this: DOI: 10.1039/c0xx00000x

www.rsc.org/xxxxxx

PAPER

# Efficacy of CNTs bound polyelectrolyte membrane by spray-assisted layer-by-layer (LbL) technique on water purification

Lei Liu<sup>a</sup>, Moon Son<sup>a</sup>, Hosik Park<sup>b</sup>, Evrim Celik<sup>c</sup>, Chiranjib Bhattacharjee<sup>d</sup>, and Heechul Choi<sup>\*a</sup>

Received (in XXX, XXX) Xth XXXXXXXXXX 20XX, Accepted Xth XXXXXXXXXX 20XX

DOI: 10.1039/b000000x

## Abstract

This study demonstrates properties of surface-modified polyethersulfone (PES) composite ultrafiltration (UF) membranes prepared by spray-assisted layer-by-layer (LbL) technique. The coating layers on PES substrate consist of polyelectrolyte multilayers (PEMs) with and without functionalized multiwall carbon nanotubes (f-MWCNTs) as the blending additive. The composite membrane acquired a negative surface charge and the hydrophilicity of the membrane increased after adding hydrophilic f-MWCNTs. The pure water permeation tests revealed that the water flux was dependent on the f-MWCNTs/polyelectrolyte weight ratio and numbers of PEMs. The prepared membrane showed slower flux reduction and lower fouling ratio ( $R_f$ ) by humic acid (HA) filtration tests. Moreover, the flux recovery ratio (FRR) after deionized (DI) water flushing was improved significantly (up to 81%) comparing with PES substrate (46%), which indicated the enhancement of anti-fouling properties. The current work presents a facile way to modify the commercial membrane surface with tuned water flux and enhanced anti-fouling properties.

## 1. Introduction

Membranes with enhanced water flux and reduced fouling tendencies are desirable in the water treatment process. In order to improve membrane performance, membrane modification has been extensively investigated, including such methods as blending, surface coating, plasma treatment, the sol-gel method, and polymerization<sup>1-7</sup>. Among various physical and chemical methodologies, tunable and facile layer-by-layer (LbL) technique serves as a potential candidate to tailor membrane with preferable properties. The resultant membranes have been employed as ultrafiltration (UF), solvent resistant nanofiltration (SRNF), and reverse osmosis (RO) membranes<sup>8-10</sup>.

The conventional LbL technique consists of an alternative deposition of positive and negative polyelectrolytes on a substrate about several minutes for each layer via a secondary force, including electrostatic, hydrophobic interaction, and hydrogen bonding. However, the traditional LbL method has disadvantages such as extended preparation time and use of large quantities of polymers. To conquer these drawbacks, spray-assisted LbL method has been employed in this study; the benign and green solvent, largely composed of de-ionized (DI) water, in the fabrication process paves the way for an environmentally-friendly technique for membrane preparation without deterioration of layer quality<sup>11-13</sup>. Poly (diallyl-dimethylammonium chloride) and Poly (sodium 4-styrenesulfonate) are two typical strong polyelectrolytes used in LbL studies<sup>14-16</sup>. However, the moieties

in LbL techniques are not limited to water-soluble polyelectrolytes; proteins, stabilized nanoparticles are also suitable as components for assembly. Chung et al. applied aquaporin-embedded LbL membrane in separation of  $MgCl_2$  and glutathione, the rejection is up to 95% and 93% respectively with enhanced water permeability<sup>17</sup>. Jones et al. and Tang et al. incorporated silver nanoparticles into the polyelectrolyte to fabricate anti-fouling membranes<sup>18, 19</sup>, and Bruening et al. introduced gold nanoparticles into polyelectrolyte to prepare catalytic membranes<sup>20</sup>.

Carbon nanotubes (CNTs) are widely used additives to strengthen the polymeric membrane properties. It has been found that the mechanical strength of the CNTs incorporated polyelectrolyte membrane was greatly improved<sup>21</sup>; additionally, our group discovered an increase in flux with CNTs blended polyethersulfone (PES) membrane<sup>1</sup>. Despite this, the agglomeration of MWCNTs via strong van der Waals forces is an obstacle toward CNTs processing and interfacial interaction with polymer matrix<sup>22</sup>, since an efficient dispersion of CNTs in solvent and polymer matrix is the prerequisite for LbL assembly and other membrane preparation processes. To assist dispersion of MWCNTs, some researchers attempted to modify CNTs using strong acid treatment<sup>23-25</sup>; the oxidized MWCNTs are shortened with open-end tips, functionalized with hydroxyl and carboxylic groups<sup>8</sup>, and several studies have proven the extraordinarily fast transport of water in open-tip CNTs<sup>26, 27</sup>. Other research groups further promote the CNTs dispersion by means of polyelectrolyte surfactant poly (sodium 4-styrenesulfonate) (PSS) wrapping on

CNTs walls through non-covalent interactions<sup>28,29</sup>.

To date, very few researches have been done in the preparation and application of functionalized multi-walled CNTs (f-MWCNTs) blended polyelectrolyte membranes in water treatment<sup>21</sup>. In this work, f-MWCNTs blended polyelectrolyte multilayers (PEMs) are deposited on commercially available PES membrane via spray-assisted LbL techniques. The composition, structure and morphology of formed membranes with different numbers of bilayers and f-MWCNTs contents were studied. Besides, to verify the hypothesis of f-MWCNTs' positive effects on membrane permeation and anti-fouling properties, the performances of the membranes towards DI water and synthetic humic acid (HA) feed solution were further tested in a custom-made cross-flow ultrafiltration apparatus. The HA was chosen as the model foulant because ultrafiltration are proven to enable the separation of HA<sup>30</sup>, and abundant HA in natural water is suggested to cause membrane fouling<sup>31</sup>.

## 2. Experimental

### 2.1 Materials

The polyethersulfone substrate (PES-SM, 20,000 Da) was obtained from Synder Filtration Inc., USA. Poly (sodium 4-styrenesulfonate) (PSS, Mw=70,000 Da, powder, Sigma-Aldrich, USA), poly (diallyl-dimethylammonium chloride) (PDDA, Mw=100,000–200,000 Da, 20 wt% in H<sub>2</sub>O, Sigma-Aldrich, USA) and humic acid (HA sodium salt, Sigma-Aldrich, USA) were used as received. MWCNTs were purchased from Hanwha Nanotech. Co. Ltd., Korea. De-ionized (DI) water (Milli-Q, 18.2 MΩ cm) was used for rinsing and solutions preparation. The experimental scheme in this study is illustrated in Fig. 1.

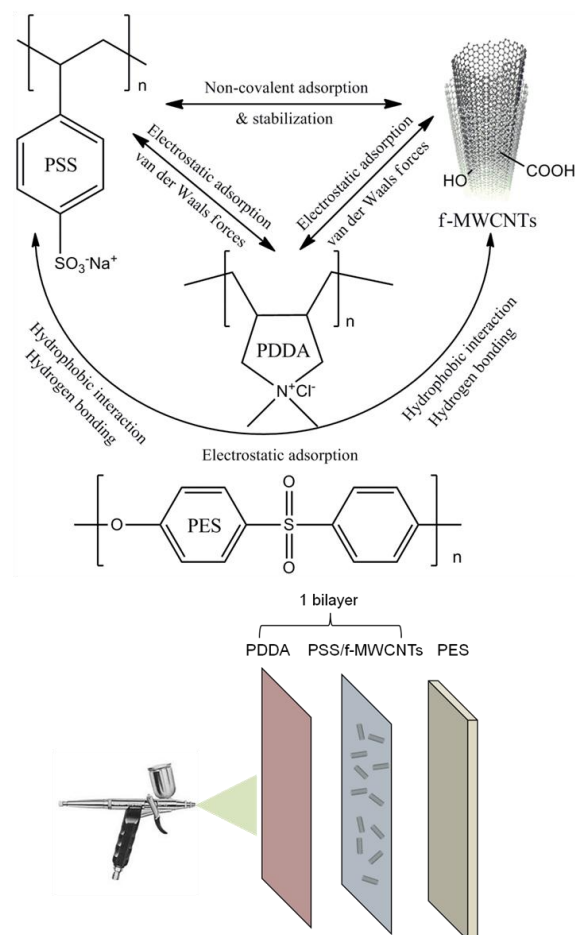


Fig. 1 The experimental scheme of this study

### 2.2 Preparation of PEMs composite membrane

Raw MWCNTs were functionalized in concentrated mixed acid (HNO<sub>3</sub>:H<sub>2</sub>SO<sub>4</sub> =3:1, v/v), the f-MWCNTs were washed by DI water and filtered using a 0.45 μm nylon filter until the pH value of the MWCNT solution reached neutral, and dried in a vacuum oven. When preparing the membrane, 1 mg/mL polycation spray solution (1 g PDDA in 1 L DI water) was prepared by adding PDDA into DI water. PSS solution was spiked into the f-MWCNTs solution with different f-MWCNTs/PSS weight ratio (1 to 10 %, w/w) to form 1 mg/mL polyanion spray solution (1 g PSS in 1 L DI water). Both the PSS and PDDA aqueous solution were prepared without adjusting pH for the reason that both polymers are strong polyelectrolytes and can be fully ionized in a wide pH range<sup>32</sup>. Pretreated PES substrate was mounted on a holder vertically with only active layer exposure to the spray solution. The spray-assisted layer-by-layer deposition of polyelectrolyte multilayers (PEMs) were completed using n cycles of polyanion spray, DI water rinse, drying by filtered air and polycation spray from an air pistol (SEIKI GP-1, 0.35 mm nozzle diameter, Japan) under 20 psi of compressed air, the spray and rinse time were 15 and 30 seconds for each layer. Hereafter, the prepared membranes are denoted as Mn-r %, the compositions of prepared membrane in this study are listed in Table 1. All membranes were freshly prepared prior to use.

**Table 1** The prepared membrane composition

Mn-r %*	Layers of polyanions (-)	Layers of polycations(+)	r %*
n*=3.5	4	3	0%, 1%, 2%, 4%, 6%, 10%
n*=6.5	7	6	0%, 1%, 2%, 4%, 6%, 10%

\*M is abbreviation for membrane, n represents the number of bilayers of f-MWCNTs/PSS-PDDA PEMs deposited on the PES, and r indicates f-MWCNTs/PSS weight ratio.

5

### 2.3 Characterization of the spray solution and the membranes

The zeta-potential and pH of the spray solution was measured by zeta potentiometer (ELS-Z, Otsuka Electronics, Japan) and pH meter (Orion 3-Star, Thermo Scientific, USA). Measurements of viscosity were performed on a rotational viscometer (Visco Elite-R, Fungilab, Spain).

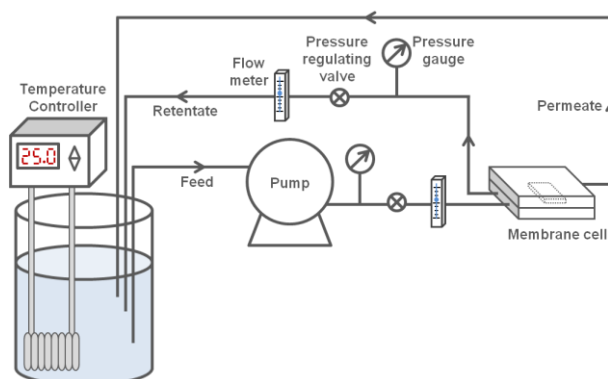
The formation of PEMs on PES substrate were verified by Fourier transform infrared-attenuated total reflectance (ATR-FTIR) spectrometer (Varian 660-IR, USA) at 4 cm<sup>-1</sup> resolution over the range of 4000–600 cm<sup>-1</sup>. The surface morphologies of the membranes were directly observed by scanning electron microscope (SEM, Hitachi S-4700, Japan). Roughness of membranes was measured by atomic force microscope (AFM, PSIA XE-100, Korea) in a contact mode with a scan size of 5 μm × 5 μm. The surface charges of the membrane at pH 7.0 were measured by zeta potentiometer (ELS-Z, Otsuka Electronics, Japan) using 1 mM NaCl as background electrolyte, the membranes were stored in background solution before measurement. The hydrophilicity of the membranes was assessed by captive bubble method on a contact angle goniometer (DSA 100, Krüss, Germany), 10 μL of air bubble was injected by the syringe and attached to the membrane surface, contact angles were measured in the DI water at room temperature.

30

### 2.4 Filtration and anti-fouling tests

The membrane permeation was evaluated using a custom-made cross-flow ultrafiltration setup. The high cross-flow rate was fixed at 400 mL/min, which can minimize the concentration polarization effect on membrane surface. The schematic configuration of the setup was shown in Fig. 2. Both permeate and retentate were circulated back to the feed tank to maintain the feed solution concentration. The effective membrane area was 18.56 cm<sup>2</sup>. All membranes were stabilized at a trans-membrane pressure (TMP) of 60 psi for 4 hours, and then the pressure was adjusted to degressive pressure from 60 psi to 10 psi as operating TMP to examine the pure water flux.

40

**Fig.2** The schematic illustration of ultrafiltration apparatus

45

For anti-fouling test, 20 mg/L HA feed solution (9.83 mgC/L-TOC, SUVA 5.05 L m<sup>-1</sup> mg<sup>-1</sup>) with or without 0.2 mM Ca<sup>2+</sup> addition was prepared by dissolving 20 mg HA into 10 mM phosphorous buffer solution (pH=7), and filtered through cellulose acetate filters (0.45 μm, Advantec, Inc. Japan). All the membranes were stabilized at TMP of 60 psi for 240 mins using DI water, then the TMP was adjusted to 50 psi, the feed solution was replaced by HA feed solution. The filtration tests were performed at 25 ± 1 °C for 480 mins, followed by 20-mins DI water flushing at a cross-flow rate of 600 mL/min for flux recovery tests.

50

The pure water flux can be calculated as

$$J = \frac{V}{A\Delta t} \quad (1)$$

where  $V$  is the volume of permeated water (L),  $A$  is effective membrane area, and  $\Delta t$  is the permeation time (h).

The flux recovery ratio ( $FRR$ ) and total flux loss  $R_t$ , which are assumed to be parameters evaluating fouling resistance of membrane<sup>8,33</sup>, are calculated using the equations:

$$FRR(\%) = \left( \frac{J_{wp}}{J_{wf}} \right) \times 100\% \quad (2)$$

$$R_t(\%) = \left( \frac{J_{wv} - J_{pf}}{J_{wv}} \right) \times 100\% \quad (3)$$

The reversible ( $R_r$ ) and irreversible ( $R_{ir}$ ) ratio are defined to further distinguish contributing factors constituting the total flux loss  $R_t$ ,

$$R_r(\%) = \left( \frac{J_{wv} - J_{pf}}{J_{wv}} \right) \times 100\% \quad (4)$$

$$R_{ir}(\%) = \left( \frac{J_{wv} - J_{wp}}{J_{wv}} \right) \times 100\% \quad (5)$$

where,  $J_{wv}$ ,  $J_{pf}$  and  $J_{wp}$  represents the flux of virgin membrane, fouled membrane after 480-min HA filtration and cleaned membrane after water flushing, respectively.

The concentration of HA in the feed and permeate is determined by UV-vis spectrometer (UV-mini 1240, Shimadzu, Japan) under 254 nm. The rejection of HA ( $R$ ) is calculated by

75

$$R\% = \frac{C_f - C_p}{C_f} \times 100\% \quad (6)$$

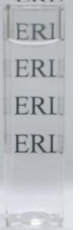


where  $C_f$ ,  $C_p$  stand for concentration of HA in the feed and permeate.

### 3 Results and discussion

#### 3.1 Effects of f-MWCNTs addition on spray solution

The physical and chemical properties of spray solution were examined before membrane fabrication and the results are listed in Table 2. As expected, the inherent zeta-potential for polycation PDDA and polyanion PSS are positive and negative. The zeta-potential of f-MWCNTs-doped PSS became more negative due to the negatively charged hydroxyl and carboxylic groups on f-MWCNTs after MWCNTs functionalization. The addition of f-MWCNTs into the solution gives more viscous and acidic spray solution. The carboxylic groups on f-MWCNTs probably contribute to pH decrease.

**Table 2** The properties of spray solution

Parameters	PDDA	PSS	PSS/CNTs
$\zeta$ potential(mV)	42.06 $\pm$ 0.16	-13.90 $\pm$ 1.08	-19.31 $\pm$ 0.47
Viscosity(Cp)	6.30 $\pm$ 0.16	6.15 $\pm$ 0.10	6.52 $\pm$ 0.08
pH	6.23 $\pm$ 0.14	5.50 $\pm$ 0.07	5.15 $\pm$ 0.06
Appearance			

#### 3.2 Characterization of membrane

##### 3.2.1 FTIR-ATR analysis

The structures of the PES substrate and prepared membranes containing PEMs fabricated from the LbL technique were studied by FTIR (Fig. 3). The absorption band at 1035  $\text{cm}^{-1}$  is attributed to symmetric  $-\text{SO}_3$  stretching vibration in PSS<sup>34</sup>. The broad band ranging from 3200 to 3600  $\text{cm}^{-1}$  is assigned to overlapping  $-\text{OH}$  and  $-\text{NH}$  stretching in f-MWCNTs and PDDA, respectively<sup>35</sup>. The FTIR spectrum confirms that f-MWCNTs contained PEMs were successfully formed onto the PES membrane layer. In addition, it is confirmed that both peak intensities are increased with more layers deposited on the PES membrane. However, the peak intensities are weaker compared to the membrane prepared using dip-coating method<sup>34</sup>, probably due to less polyelectrolyte adsorption by the relatively short spray time (15 seconds).

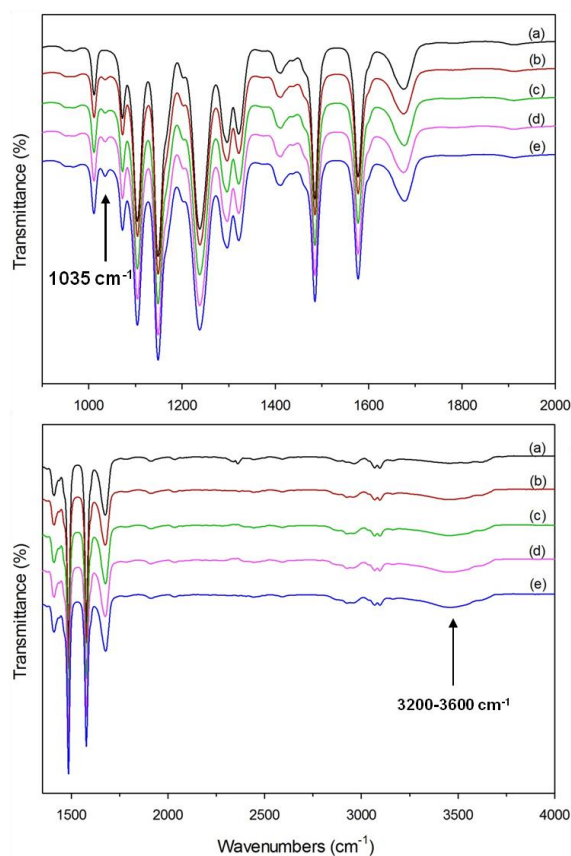


**Fig.3** FTIR-ATR spectrum of bare and prepared membranes. (a) PES substrate; (b) M3.5-0 %; (c) M6.5-0 %; (d) M3.5-4 %; (e) M6.5-4 %

##### 3.2.2 Morphology of the membranes

The SEM images of membranes before and after surface modification are illustrated in Fig. 4. For M3.5-0 % (Fig. 4c, 4d) and M6.5-0 % (Fig. 4e, 4f), there are no apparent morphology changes after PEMs deposited. While for M3.5-4 % (Fig. 4g, 4h) and M6.5-4 % (Fig. 4i, 4j), it is clearly seen that the membranes are distributed with shortened f-MWCNTs throughout the surface and embedded into the polymer matrix. M6.5-4 % exhibits more f-MWCNTs content as compared with M3.5-4 %. The thickness of PEMs of M3.5-4 % and M6.5-4 % are 44 nm and 85 nm, provided by Fig. 4k and 4l. As can be seen from the inset of Fig. 4a, the thickness of PES finger-shape cross section is about 68  $\mu\text{m}$ , so the PEMs can be defined as ultra-thin layer with respect to the PES substrate. In virtue of CNTs functionalization and PSS-assisted dispersion, no aggregations occurred based on the observation of SEM images.

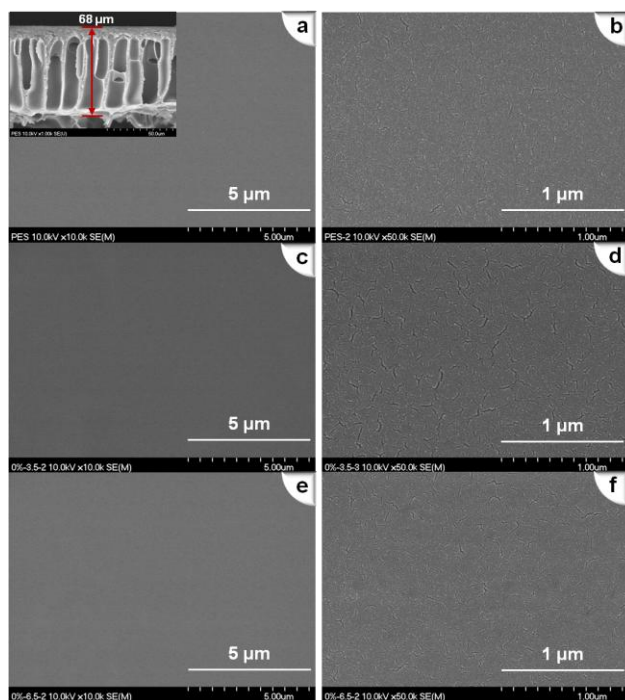


**Fig.4** SEM images of prepared membrane (a)-(j) top view, (k)(l) cross section; (a)(b) PES substrate; (c)(d) M3.5-0 %; (e)(f) M6.5-0 %; (g)(h) M3.5-4 %; (i)(j) M6.5-4 %; (k) M3.5-4 %; (l) M6.5-4 %

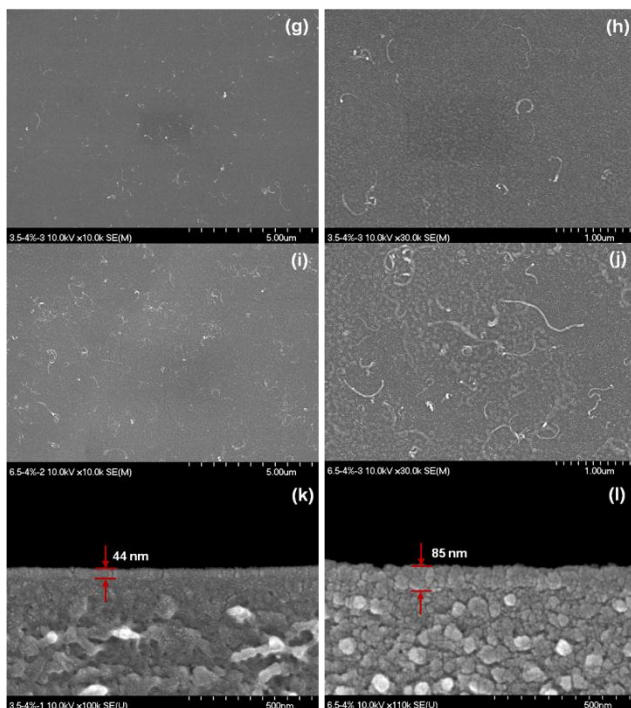


**Fig.4(continued)** SEM images of prepared membrane (a)-(j) top view, (k)(l) cross section; (a)(b) PES substrate; (c)(d) M3.5-0 %; (e)(f) M6.5-0 %; (g)(h) M3.5-4 %; (i)(j) M6.5-4 %; (k) M3.5-4 %; (l) M6.5-4 %

The surface roughness is represented by AFM root mean square (RMS) values. Following surface modification, RMS values and images in Fig. 5 and Fig. 6 depict rougher surfaces. After surface modification of PES substrate, the roughness of Mn-0 % is increased, which is consistent with previous researches<sup>36, 37</sup>. As discussed in section 3.3, this behavior is caused by loopy

15 conformation of PEMs in the absence of f-MWCNTs. For Mn-4 %, roughness correlates with the presence of f-MWCNTs, whereas M6.5-4 % shows a slightly rougher surface than M3.5-4 %. It is noted that the surface of Mn-4 % appears not as rough as expected, most of f-MWCNTs are embedded in the PEMs  
20 matrix owes to the f-MWCNTs' stronger attractive interactions with PEMs on PES substrate.

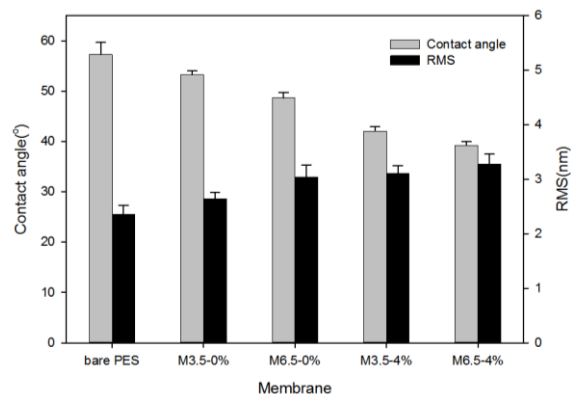


**Fig.5** Contact angle and roughness of prepared membranes

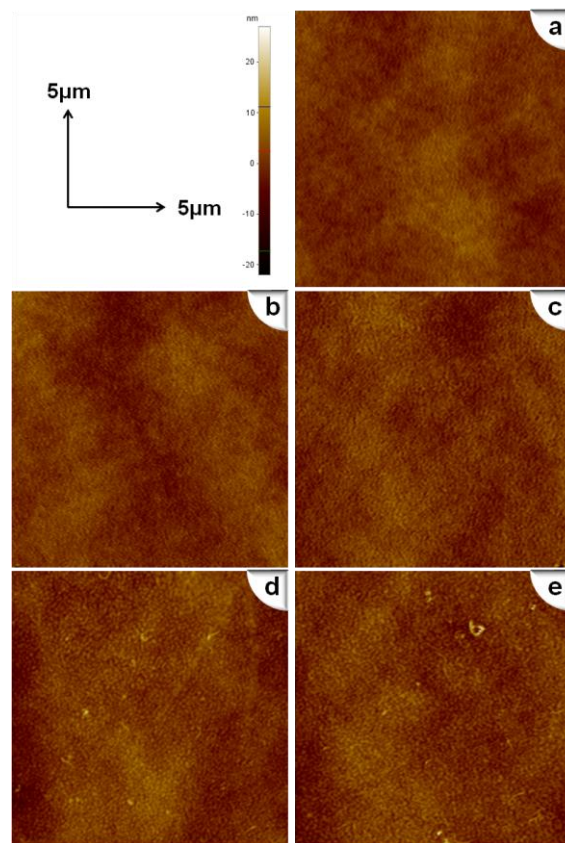


**Fig.6** AFM images of prepared membranes (a) PES substrate; (b) M3.5-0 %; (c) M6.5-0 %; (d) M3.5-4 %; (e) M6.5-4 %

### 3.2.3 Hydrophilicity of the membranes

Captive bubble method is adopted for contact angle measurements since it gives more accurate results for hydrophilic membrane surface<sup>38</sup>, and the results are presented in Fig. 5. The membranes terminated with PSS layer have lower contact angle values than unmodified PES substrate, suggesting that the

membrane become more hydrophilic. In agreement with previous studies, the hydrophilicity of the membrane further increased with addition of f-MWCNTs<sup>1,33</sup>, Mn-4 % are more hydrophilic than Mn-0 % and PES substrate, surface coating decreased the contact angle from 57° for bare membrane to 39° after 6.5 bilayer PEM coating, the hydrophilic hydroxyl and carboxylic groups on f-MWCNTs probably result in the decrease of the contact angles<sup>1,39</sup>. More hydrophilic surface makes the membrane less susceptible to fouling.

#### 3.2.4 The surface charge of the membrane

The zeta-potential of bare PES membrane and Mn-0 % under pH of 7.0 in 1 mM NaCl were reported in Fig.S1. The bare membrane has a negative zeta-potential of -24 mV, after 3.5 and 6.5 bilayer PEMs coating, the zeta potential values shift to -36 and -52 mV for M3.5-0 % and M6.5-0 %, respectively. Even though the intrinsic electrical conducting properties of MWCNTs in PEMs affected the zeta-potential measurement<sup>1</sup>, one can hypothesize more negative zeta-potential values for M3.5-4 % and M6.5-4 %, which is induced by f-MWCNTs-doped PSS spray solution (Table 2). The membrane with more negatively charged surface is required for anti-fouling properties.

### 3.3 Effects of f-MWCNTs on membrane filtration properties

For the purpose of finding the f-MWCNTs/PSS ratio imparting the changes of water flux, a series of ratios initiated from 1 % (w/w) were tested and the results are displayed in Fig. 7a and 7b. Up to 4 % (w/w) of f-MWCNTs/PSS ratio, both M3.5-r % and M6.5-r % membrane showed increased water flux with the weight ratio r increases. These results are probably due to the hydrophilicity enhancement of the membrane<sup>40</sup> and the interior voids formation between f-MWCNTs and polymer chains<sup>41</sup>. It was also found that M6.5-0 % shows more significant flux reduction than M3.5-0 %, similar trends were found in other M6.5-r % and M3.5-r % membranes, which is caused by thicker PEM deposited on PES substrate, whereas M6.5-r % exhibits a faster flux enhancement than M3.5-r % as the ratio r increases. However, the flux reached a plateau for M3.5-r %, in contrast to sharp declines for M6.5-r % when the f-MWCNTs/PSS ratio was over 4 % (w/w). This indicates the insufficient PSS presence to wind and disperse the CNTs as the amount of CNTs increase, eventually partial aggregations of the CNTs fail to effectively facilitate the water molecules in the PEMs<sup>42</sup>.

Fig. 7c, 7d shows the linear relationship between pure water flux versus trans-membrane pressure. Flux of membranes containing f-MWCNTs is higher than that of membrane without f-MWCNTs in PEMs. As aforementioned, the membranes containing f-MWCNTs are more hydrophilic, which is pronounced for water flux enhancement. Furthermore, these f-MWCNTs introduce more free voids between polymer chains<sup>41</sup>, and the f-MWCNTs may act as the channels for water molecules to pass easily. Consequently, M6.5-4 % shows relatively higher incremental enhancement according to pressure changes. Besides, without negatively charged f-MWCNTs in PSS solution, the intra-chain electrostatic repulsion forces between PSS polymer chains are relatively small, there is less conformational change from a random coiled structure to a linear structure, which results in a

thick and loopy structure of PEMs formed on PES substrate for M3.5-0 % and M6.5-0 %<sup>43</sup>, finally lead to lower flux. The PEMs depositions ensure the MWCO of PES substrate below 20 kDa, which is beneficial for the separation of smaller molecules in water treatment without mitigating the water flux due to the ultra-thin PEMs.

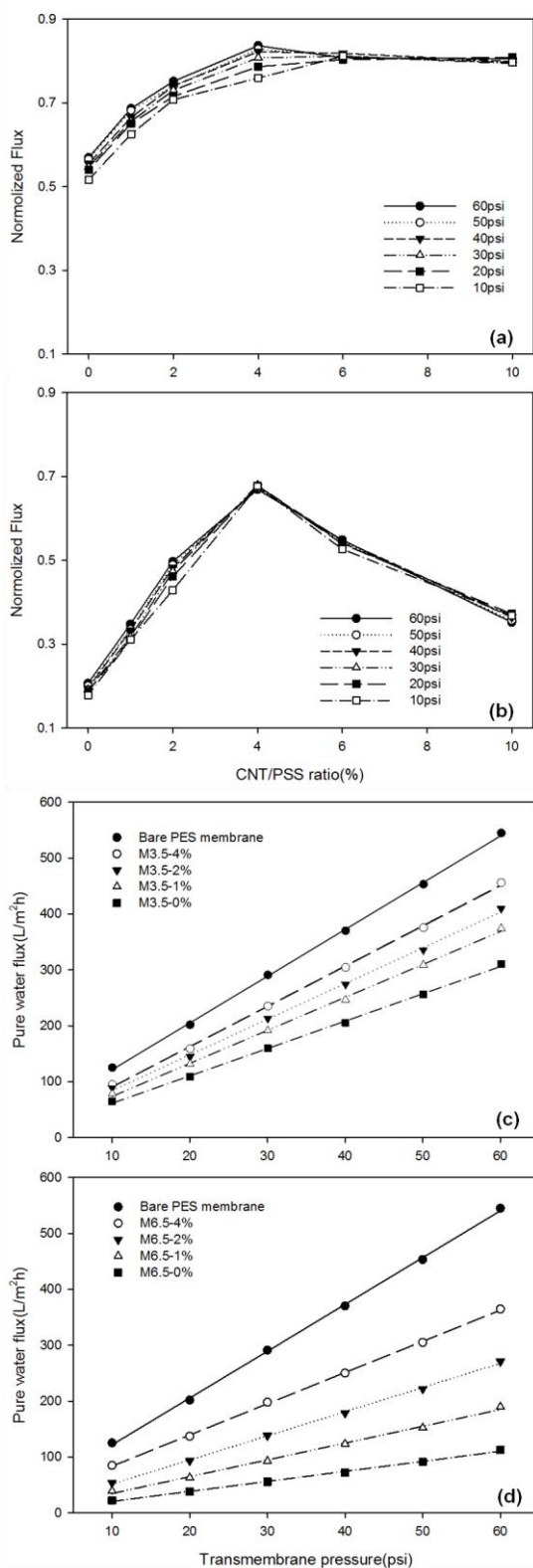


**Fig.7** Pure water flux depending on (a) f-MWCNTs/PSS ratio of 3.5 bilayer membrane; (b) f-MWCNTs/PSS ratio of 6.5 bilayer membrane; (c) TMP of 3.5 bilayer membrane; (d) TMP of 6.5 bilayer membrane

### 3.4 Anti-fouling properties of the membrane

To assess the effects of different surface properties on HA fouling, bare PES membrane, M3.5-4 % and M6.5-4 % were chosen for anti-fouling tests. The decline in flux for three types of membrane was shown in Fig. 8a. Membrane surface modification significantly slowed the rate of flux decline. Fig. 8b shows the adverse effect of Ca<sup>2+</sup> ion addition on membrane fouling by HA. The flux decline was more severe for all three types of membranes. This is mainly due to the dense HA layer on negatively charge membrane surface via calcium-HA complexation. An apparent comparison of membrane surface after 20-min DI water flushing is also illustrated in Fig. S2.

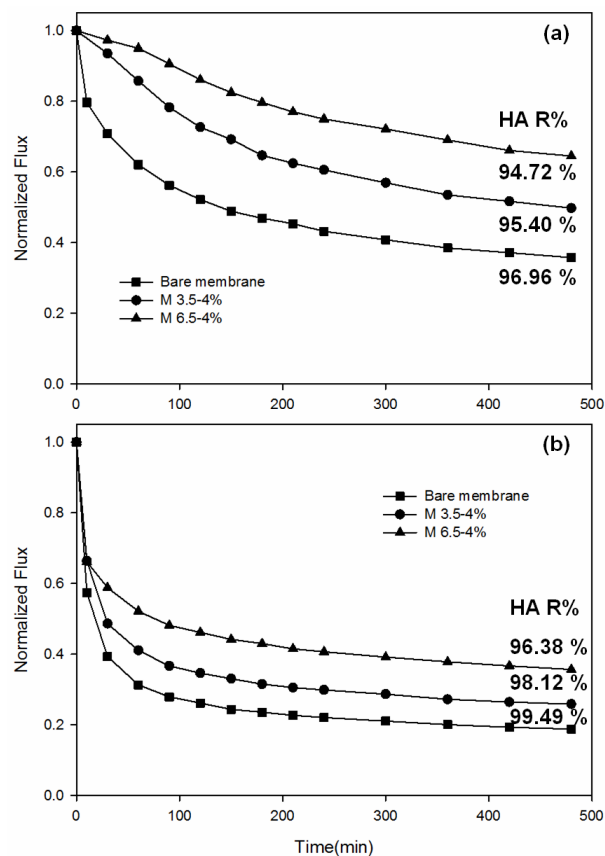


**Fig.8** Humic acid filtration test with prepared membrane (a) 20 mg/L humic acid without Ca<sup>2+</sup>; (b) 20 mg/L humic acid with 0.2 mM Ca<sup>2+</sup> at 25 °C under 50 psi TMP

The difference in fouling patterns relies mainly on membrane surface properties, which is illustrated by fouling resistance ( $R_f$ ) and flux recovery ratio ( $FRR$ ) in Fig. 9. The  $R_f$  of M6.5-4 % is 35 % after HA filtration, which is superior to those of M3.5-4 % and bare PES membrane.  $FRR$  for M6.5-4 % reaches up to 81 % after applying 20-min DI water flushing. The HA is negatively-charged in feed solution with pH 7.0 due to the deprotonation of carboxylic, hydroxyl and phenolic groups bearing in it<sup>44</sup>; The HA SUVA value over 4 means the hydrophobic aromatic compounds with high molecular weight prevails<sup>45</sup>. Thus, surface modification of PES substrate maximize the electrostatic repulsion and minimize the hydrophobic interaction between HA and membrane surface, which caused HA fouling prevention.

5



Even though the presence of  $\text{Ca}^{2+}$  ion inevitably shield the charge on the HA, induce stretched and linear HA into coiled and compact configuration, then increase the adsorption on the membrane surface with irreversible fouling<sup>30</sup>, the prepared membrane showed improved anti-HA fouling properties as well as rejection shown in Fig 8.

It is also interesting to note that, usually a rougher surface increases the chance of fouling due to easy foulants accumulation; however, the surface modified membranes with somehow rougher surface exhibit improved anti-fouling properties in this test. Therefore, surface charge or hydrophilicity plays an important role for HA fouling reduction, which is in line with the conclusions drawn by another study<sup>46</sup>.

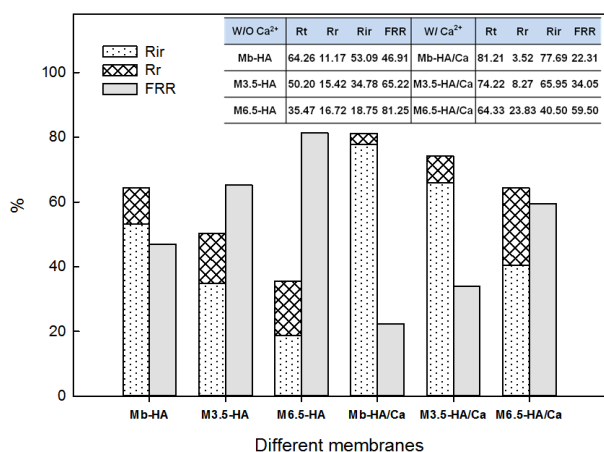


**Fig.9** Fouling ratios of the prepared membrane for humic acid filtration test,  $FRR$ ,  $R_r$ ,  $R_r$ ,  $R_{ir}$  stands for the flux recovery ratio, total flux loss, the reversible ratio and irreversible ratio, respectively.

## Conclusions

In conclusion, our studies presented a series of ultrafiltration membrane composed of f-MWCNTs blended ultra-thin polyelectrolyte layer as active layer on commercial PES membrane prepared by spray-assisted LbL techniques. Successful preparations were proved through characterization results. An array of membranes with multiple f-MWCNTs/PSS weight ratios and numbers of deposited bilayers were tested under ultrafiltration conditions. The above-discussed results confirm the positive effects of f-MWCNTs on water flux enhancement, and 4% f-MWCNTs/PSS weight ratio is the optimal for both 3.5 and 6.5 bilayer PEMs membranes, which probably ascribes to the hydrophilicity enhanced by f-MWCNTs, free voids generated between f-MWCNTs and polymer; f-MWCNTs may also contribute to rapid water molecules transport as open-tip channels. The fouling patterns by HA depend principally on membrane surface physical and chemical properties, the improved anti-HA fouling properties manifest the potential applications of CNTs blended polyelectrolyte membrane in water treatment.

## Acknowledgements

This work was supported by the National Research Foundation of Korea (NRF) grant funded by the Korea government (MEST) (No. 2011-0027712 and No. 2012R1A2A2A03046711) and "Basic Research Projects in High-tech Industrial Technology" Project through a grant provided by GIST in 2013.

## Notes and references

<sup>a</sup> School of Environmental Science and Engineering, Gwangju Institute of Science and Technology (GIST), 261 Cheomdan-gwagiro, 1 Oryong-dong, Buk-gu, Gwangju 500712, Republic of Korea. Fax: +82 62 7152434; Tel: +82 62 7152576; E-mail: hcchoi@gist.ac.kr

<sup>b</sup> Research Center for Environmental Resources and Processes, Korea Research Institute of Chemical Technology (KRICT), Daejeon 305600, Republic of Korea.

<sup>c</sup> Department of Environmental Engineering, Faculty of Engineering, Suleyman Demirel University, Isparta 32260, Turkey.

<sup>d</sup> Department of Chemical Engineering, Jadavpur University, 188, Raja Subodh Chandra Mullick Road, Kolkata 700032, India.

† Electronic Supplementary Information (ESI) available:

Fig. S1 Zeta potential of bare and surface-modified membranes with different number of bilayers.

Fig. S2 The fouled membrane by 20 mg/L humic acid after 20 mins DI water flushing (a) bare membrane, (b) M3.5-4%, (c) M6.5-4% without  $\text{Ca}^{2+}$ ; (d) bare membrane, (e) M3.5-4%, (f) M6.5-4% with 0.2 mM  $\text{Ca}^{2+}$ .

See DOI: 10.1039/b000000x/

1. E. Celik, H. Park, H. Choi and H. Choi, *Water Res.*, 2011, **45**, 274-282.
2. V. Vatanpour, S. S. Madaeni, L. Rajabi, S. Zinadini and A. A. Derakhshan, *J. Membr. Sci.*, 2012, **401-402**, 132-143.
3. J. Kochan, T. Wintgens, J. E. Wong and T. Melin, *Desalin. Water Treat.*, 2009, **9**, 175-180.
4. F. Zhang, W. Zhang, Y. Yu, B. Deng, J. Li and J. Jin, *J. Membr. Sci.*, 2013, **432**, 25-32.
5. D.G. Kim, H. Kang, S. Han, H. J. Kim and J.C. Lee, *RSC Adv.*, 2013, **3**, 18071-18081.
6. B. Zhang, L. Liu, S. Xie, F. Shen, H. Yan, H. Wu, Y. Wan, M. Yu, H. Ma, L. Li and J. Li, *RSC Adv.*, 2014, **4**, 16561-16566.
7. C. Cheng, L. Ma, D. Wu, J. Ren, W. Zhao, J. Xue, S. Sun and C. Zhao, *J. Membr. Sci.*, 2011, **378**, 369-381.
8. L. Liu, M. Son, S. Chakraborty, C. Bhattacharjee and H. Choi, *Desalin. Water Treat.*, 2013, **51**, 6194-6200.
9. P. Ahmadiannamini, X. Li, W. Goyens, N. Joseph, B. Meesschaert and I. F. J. Vankelecom, *J. Membr. Sci.*, 2012, **394-395**, 98-106.
10. J. Park, J. Park, S. H. Kim, J. Cho and J. Bang, *J. Mater. Chem.*, 2010, **20**, 2085-2091.
11. J. B. Schlenoff, S. T. Dubas and T. Farhat, *Langmuir*, 2000, **16**, 9968-9969.
12. M. Kolasinska, R. Krastev, T. Gutberlet and P. Warszynski, *Langmuir*, 2008, **25**, 1224-1232.
13. M. Bruening and D. Dotzauer, *Nat. Mater.*, 2009, **8**, 449-450.
14. B. P. Tripathi, N. C. Dubey and M. Stamm, *J. Hazard. Mater.*, 2013, **252-253**, 401-412.
15. N. Ladhari, J. Hemmerlé C. Ringwald, Y. Haikel, J. C. Voegel, P. Schaaf and V. Ball, *Colloid Surf. A-Physicochem. Eng. Asp.*, 2008, **322**, 142-147.
16. L. Ouyang, R. Malaisamy and M. L. Bruening, *J. Membr. Sci.*, 2008, **310**, 76-84.
17. G. Sun, T. S. Chung, K. Jeyaseelan and A. Armugam, *RSC Adv.* 2013, **3**, 473-481.
18. F. Diagne, R. Malaisamy, V. Boddie, R. D. Holbrook, B. Eribo and K. L. Jones, *Environ. Sci. Technol.*, 2012, **46**, 4025-4033.
19. X. Liu, S. Qi, Y. Li, L. Yang, B. Cao and C. Y. Tang, *Water Res.*, 2013, **47**, 3081-3092.

20. D. M. Dotzauer, J. Dai, L. Sun and M. L. Bruening, *Nano Lett.*, 2006, **6**, 2268-2272.
21. Q. Zhao, J. Qian, M. Zhu and Q. An, *J. Mater. Chem.*, 2009, **19**, 8732-8740.
- 5 22. P. C. Ma, N. A. Siddiqui, G. Marom and J. K. Kim, *Compos. Part A - Appl. S.*, 2010, **41**, 1345-1367.
23. T. Saito, K. Matsushige and K. Tanaka, *Physica B*, 2002, **323**, 280-283.
24. F. Avilés, J. V. Cauich-Rodríguez, L. Moo-Tah, A. May-Pat and R. Vargas-Coronado, *Carbon*, 2009, **47**, 2970-2975.
- 10 25. J. Liu, A. G. Rinzler, H. Dai, J. H. Hafner, R. K. Bradley, P. J. Boul, A. Lu, T. Iverson, K. Shelimov, C. B. Huffman, F. Rodriguez-Macias, Y.-S. Shon, T. R. Lee, D. T. Colbert and R. E. Smalley, *Science*, 1998, **280**, 1253-1256.
- 15 26. H. Verweij, M. C. Schillo and J. Li, *Small*, 2007, **3**, 1996-2004.
27. S. Joseph and N. R. Aluru, *Nano Lett.*, 2008, **8**, 452-458.
28. S. Zhan and Y. Li, *J. Dispers. Sci. Technol.*, 2008, **29**, 240-244.
29. C. Iamsamai, A. Soottitawat, U. Ruktanonchai, S. Hannongbua and S. T. Dubas, *Carbon*, 2011, **49**, 2039-2045.
- 30 30. D. Jermann, W. Pronk, S. Meylan and M. Boller, *Water Res.*, 2007, **41**, 1713-1722.
31. X. Cui and K. Choo, *Environ. Eng. Res.*, 2014, **19**, 1-8.
32. P. Ahmadiannamini, X. Li, W. Goyens, B. Meesschaert and I. F. J. Vankelecom, *J. Membr. Sci.*, 2010, **360**, 250-258.
- 33 33. E. Celik, L. Liu and H. Choi, *Water Res.*, 2011, **45**, 5287-5294.
34. A. V. R. Reddy, D. J. Mohan, A. Bhattacharya, V. J. Shah and P. K. Ghosh, *J. Membr. Sci.*, 2003, **214**, 211-221.
35. S. Deng and Y. P. Ting, *Water Res.*, 2005, **39**, 2167-2177.
36. R. Hadj Lajimi, E. Ferjani, M. S. Roudesli and A. Deratani, *Desalination*, 2011, **266**, 78-86.
- 30 37. T. Zhang, H. Gu, P. Qin and T. Tan, *Ind. Eng. Chem. Res.*, 2013, **52**, 6517-6523.
38. W. Zhang, M. Wahlgren and B. Sivik, *Desalination*, 1989, **72**, 263-273.
- 35 39. S. Majeed, D. Fierro, K. Buhr, J. Wind, B. Du, A. Boschetti-de-Fierro and V. Abetz, *J. Membr. Sci.*, 2012, **403-404**, 101-109.
40. S. Roy, S. A. Ntim, S. Mitra and K. K. Sirkar, *J. Membr. Sci.*, 2011, **375**, 81-87.
41. A. F. Ismail, P. S. Goh, S. M. Sanip and M. Aziz, *Sep. Purif. Technol.*, 2009, **70**, 12-26.
- 40 42. C. Tang, Q. Zhang, K. Wang, Q. Fu and C. Zhang, *J. Membr. Sci.*, 2009, **337**, 240-247.
43. P. Ahmadiannamini, X. Li, W. Goyens, B. Meesschaert, W. Vanderlinden, S. De Feyter and I. F. J. Vankelecom, *J. Membr. Sci.*, 2012, **403-404**, 216-226.
- 45 44. T. S. Anirudhan and P. S. Suchithra, *Chem. Eng. J.*, 2010, **156**, 146-156.
45. Z. Yigit and H. Inan, *Water Air Soil Pollut: Focus*, 2009, **9**, 237-243.
46. L. Yan, Y. S. Li, C. B. Xiang and S. Xianda, *J. Membr. Sci.*, 2006, **276**, 162-167.
- 50